Space Weather

RESEARCH ARTICLE
10.1029/2018SW001894

Geoeffectiveness of Stream Interaction Regions From 1995 to 2016

Yutian Chi[1], Chenglong Shen[1,2,3], Bingxian Luo[4,5], Yuming Wang[1,6], and Mengjiao Xu[1,3]

[1]CAS Key Laboratory of Geospace Environment, Department of Geophysics and Planetary Sciences, University of Science & Technology of China, Hefei, China, [2]CAS Center for Excellence in Comparative Planetology, University of Science and Technology of China, Hefei, China, [3]Mengcheng National Geophysical Observatory, School of Earth and Space Sciences, University of Science and Technology of China, Hefei, China, [4]National Space Science CenterChinese Academy of Sciences, Beijing, China, [5]School of Astronomy and Space ScienceUniversity of Chinese Academy of Sciences, Beijing, China, [6]Collaborative Innovation Center of Astronautical Science and Technology, Hefei, China

Key Points:
- The near-Earth SIR catalog developed by Jian et al. (2006) has been extended to the end of 2016
- Fifty-two percent of the SIRs caused geomagnetic storms, but only 3% of the SIRs caused intense geomagnetic storms
- SIRs that interact with ICMEs exhibit significantly enhanced geoeffectiveness

Supporting Information:
- Supporting Information S1
- Table S1
- Table S2
- Text S1

Correspondence to:
C. Shen,
clshen@ustc.edu.cn

Citation:
Chi, Y., Shen, C., Luo, B., Wang, Y., & Xu, M. (2018). Geoeffectiveness of stream interaction regions from 1995 to 2016. *Space Weather*, *16*, 1960–1971. https://doi.org/10.1029/2018SW001894

Received 11 APR 2018
Accepted 10 NOV 2018
Accepted article online 16 NOV 2018
Published online 7 DEC 2018

Abstract Stream interaction regions (SIRs) are important sources of geomagnetic storms. In this work, we first extend the end time of the widely used SIR catalog developed by Jian et al. (2006, https://doi.org/10.1007/s11207-006-0132-3), which covered the period from 1995 to 2009, to the end of 2016. Based on this extended SIR catalog, the geoeffectiveness of SIRs is discussed in detail. It was found that 52% of the SIRs caused geomagnetic storms with $Dst_{min} \leq -30$ nT, but only 3% of them caused intense geomagnetic storms with $Dst_{min} \leq -100$ nT. Furthermore, we found that 10 of the intense geomagnetic storms caused by SIRs were associated with complex structures due to interactions between SIRs and interplanetary coronal mass ejections (ICMEs). In such a structure, an ICME is embedded in the SIR and located between the slow and fast solar wind streams. In addition, we found that the geoeffectiveness of SIRs interacting with ICMEs is enhanced. The possibility of SIR-ICME interaction structures causing geomagnetic storms is markedly higher than that of isolated SIRs or isolated ICMEs. In particular, the geoeffectiveness of SIR-ICME interaction structures is similar to that of the Shock-ICME interaction structures, which have been demonstrated to be the main causes of geomagnetic storms.

1. Introduction

Geomagnetic storms are one of the major space weather hazards and may significantly influence communication systems, electric power transmission systems, and GPS-based navigation systems (e.g., Astafyeva et al., 2014; Kappenman, 2005; Lucas et al., 2018; Thomson et al., 2005, and references therein). Thus, the analysis and forecasting of geomagnetic storms is an important issue in the space weather community. In the forecasting of events related to geomagnetic storms, the following questions must be answered. (1) Will a geomagnetic storm happen, and if so, when? (2) What will be the intensity of the geomagnetic storm? (3) How will the geomagnetic storm influence our space environment? Currently, the most widely used methods to forecast geomagnetic storms are based on the input of the in situ solar wind and magnetic field observations recorded at the Sun-Earth L1 point. Using these parameters, different models have been developed to forecast the geomagnetic activity index (e.g., O'Brien & McPherron, 2000; Temerin & Li, 2002; Wang et al., 2003). Those models can well forecast the geomagnetic activity indices. However, the transit time of the interplanetary structures between arriving at the L1 point and actually affecting Earth is approximately 1 hr. Thus, these models can forecast geomagnetic storms in advance by 1 hr. To make an earlier forecast, we have to know more about the solar and interplanetary origins of geomagnetic storms. The questions we need to answer include the following. What are the sources of geomagnetic storms? What are the probabilities of these structures causing geomagnetic storms? Is there any process that could influence the geoeffectiveness of these structures?

The intensity of a geomagnetic storm can be described by the disturbance storm time (*Dst*) index. The *Dst* index shows the H-component perturbation on equatorial magnetometers and was initiated more than 60 years ago (e.g., Borovsky & Shprits, 2017; Mayaud, 2013, and references therein). Using minimum values of the *Dst* indices (Dst_{min}) of geomagnetic storms, intensities of geomagnetic storms can be described in different levels, such as minor geomagnetic storms (-50 nT $< Dst_{min} \leq -30$ nT), moderate geomagnetic storms (-100 nT $< Dst_{min} \leq -50$ nT) and intense geomagnetic storms ($Dst_{min} \leq -100$ nT; e.g., Gonzalez et al., 1994).

Interplanetary coronal mass ejections (ICMEs) and stream interaction regions (SIRs) are two important interplanetary sources of geomagnetic storms (e.g., Gonzalez et al., 1994, 1999). ICMEs are the interplanetary counterparts of coronal mass ejections (CMEs), which have been widely studied for decades (e.g., Burlaga et al., 1981, 2001; Cane & Richardson, 2003; Chi et al., 2016; Gopalswamy, 2006; Gosling et al., 1973; Jian et al., 2006, 2011; Kilpua et al., 2009, 2012, 2014, 2017; Owens, 2005; Richardson & Cane, 2010; Wimmer-Schweingruber et al., 2006, and references therein). Previous results have suggested that ICMEs are the major sources of intense geomagnetic storms (e.g., Echer et al., 2013; Gonzalez et al., 1994, 1999; Shen et al., 2017; Zhang et al., 2007). Zhang et al. (2007) found that 87% of intense geomagnetic storms were caused by ICMEs. This result has been further confirmed by Shen et al. (2017). However, for moderate geomagnetic storms with -100 nT $< Dst \leq -50$ nT, the interplanetary sources might be different. Echer et al. (2013) found that only approximately 21% of moderate geomagnetic storms were caused by ICMEs, and half were caused by SIRs and high-speed streams (HSSs). SIRs are caused by the interactions between the fast solar wind streams originating from coronal holes (CHs) and slow solar wind streams (e.g., Balogh & Erdős, 2013; Gosling & Pizzo, 1999; Jian et al., 2006, 2008, and references therein), and they play a very important role in solar wind dynamics (González-Esparza & Smith, 1996). If SIRs recur on successive solar rotations, they are commonly called corotating interaction regions (CIRs; e.g., Gosling & Pizzo, 1999). SIRs are thought to be the major drivers of moderate geomagnetic storms (e.g., Echer et al., 2013; Shen et al., 2017; Zhang et al., 2006, and references therein). From another point of view, the geoeffectiveness of SIRs has also been widely studied by different authors (e.g., Alves et al., 2006; Kilpua et al., 2017; Lockwood et al., 2016; Sanchez-Garcia et al., 2017; Zhang et al., 2008). Using solar wind observations during the period from 1964 to 2003, Alves et al. (2006) found that 33% of SIRs were followed by moderate/intense magnetic activity ($Dst \leq -50$ nT). Using the Hakamada-Akasofu-Fry model, Zhang et al. (2008) identified SIRs and found that 82% of pure SIRs from 1996 to 2005 caused geomagnetic storms. Lockwood et al. (2016) showed that small-scale solar wind structures and SIRs generated as many hours of the strong southward interplanetary magnetic field as ICMEs. They further suggested that SIRs had a greater geomagnetic effect than expected. Sanchez-Garcia et al. (2017) studied the geoeffectiveness of SIRs during 2007 and 2008. They found that the percentage of SIRs causing geomagnetic storms was 50%, 55%, and 90% using the criteria of the aa, Kp, and equivalent symmetric disturbance component in H (SYM-H) indices, respectively.

In this work, we first extend the time period of the SIR catalog to the end of 2016 and then study the geoeffectiveness of SIRs in detail for a long period from 1995 to 2016, covering approximately two solar cycles. In section 2, we introduce the method that we used to obtain the extended version of the SIR catalog. The geoeffectiveness of SIRs is discussed in section 3. In section 4, we show the influence of SIR-ICME interaction on the geoeffectiveness. In the last section, we give the results and provide a brief discussion.

2. Data Selection

Two online SIR catalogs were established by Jian using the Wind and Advanced Composition Explorer (ACE) observations (Jian et al., 2006; http://www-ssc.igpp.ucla.edu/~jlan/ACE/Level3/SIR_List_from_Lan_Jian.pdf) and the Solar TErrestrial RElations Observatory (STEREO) observations (Jian et al., 2013). In these catalogs, the increasing solar wind speed and total pressure (P_t) at its maximum are two necessary criteria to determine the SIRs (e.g., Jian et al., 2006, 2013). In addition, the compressed proton number density, compressed magnetic field at the interface, flow deflection, and temperature increase at the interface are other signatures used to identify possible SIR structures. We cannot assess the geoeffectiveness of the events in Jian's STEREO SIR catalog, because those events were far from Earth. Thus, for the two existing catalogs, we only consider the SIRs obtained by Wind/ACE observations. It is worth noting that the open published Wind/ACE SIR catalog developed by Jian (hereafter, the JL catalog) only covers the period from 1995 to 2009. Based on their website, this catalog was last updated in 2014 to refine detail.

To study the geoeffectiveness of SIRs over a longer time period, we first extend the near-Earth-observed SIR catalog to the end of 2016 based on the interplanetary magnetic field and solar wind plasma observations from the Wind satellite. The criteria we used to identify the SIRs are the same as Jian et al. (2006, 2013). Figure 1 illustrates a typical SIR event recorded by the Wind spacecraft on 28–30 January 1995. The blue vertical lines in this figure show the beginning and end times of the SIR. The compressed magnetic field,

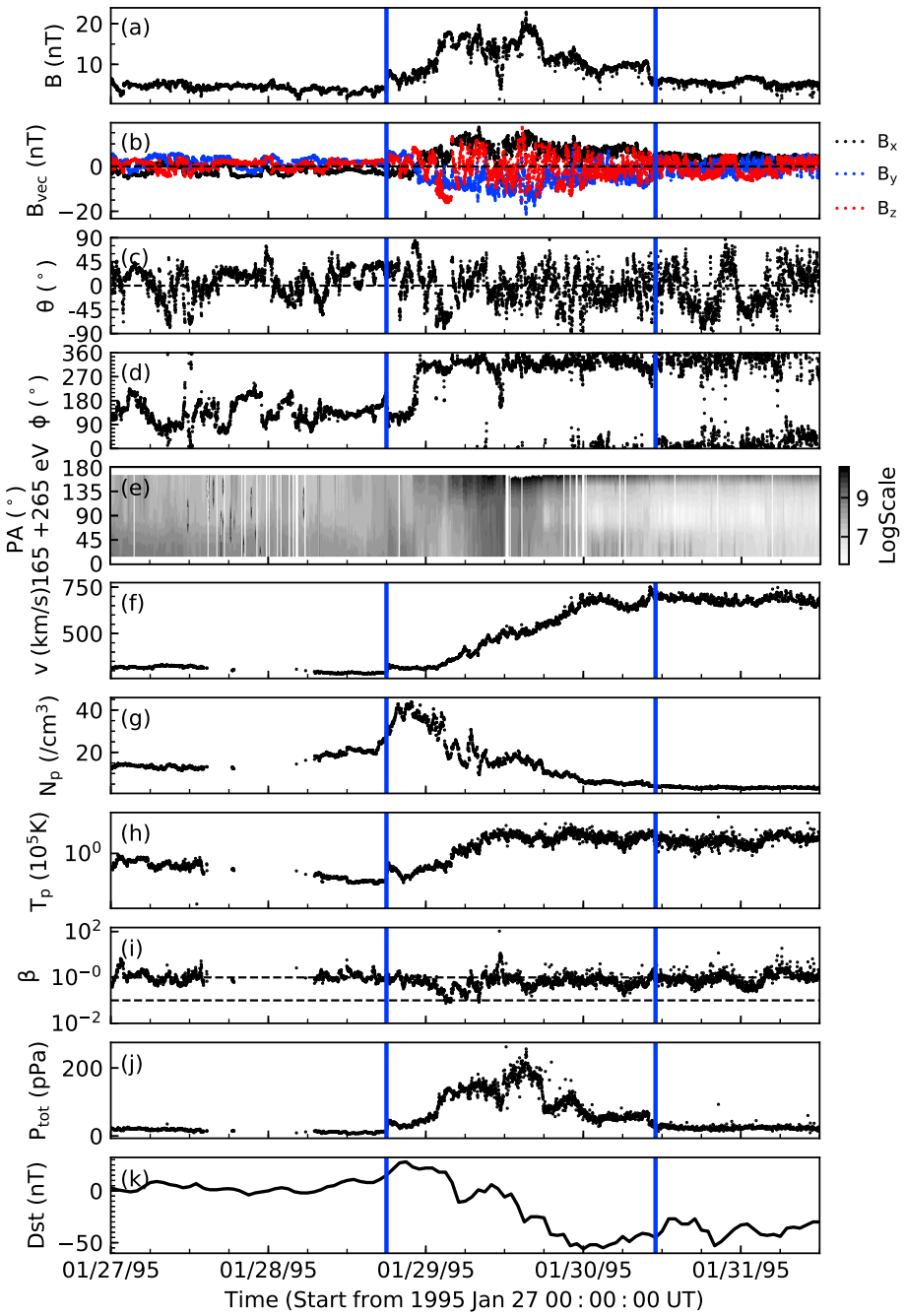

Figure 1. The interplanetary observations of a typical SIR event: 28 January 1995 event. From top to bottom, panels are the (a) magnetic field strength (B), (b) three components of the magnetic field in GSM coordinate system (B_x, B_y, and B_z), (c) the elevation (θ) and (d) azimuthal (ϕ) of magnetic field direction in GSM coordinate system, (e) the suprathermal electron pitch angle distribution, (f) solar wind speed (v), (g) proton density (N_p), (h) proton temperature (T_p), (i) the ratio of proton thermal pressure to magnetic pressure (β), (j) the total pressure and (k) the *Dst* indices from WDC. The blue vertical lines show the beginning and end time of the SIR. SIR = stream interaction region; GSM = geocentric solar magnetospheric; WDC = World Data Center.

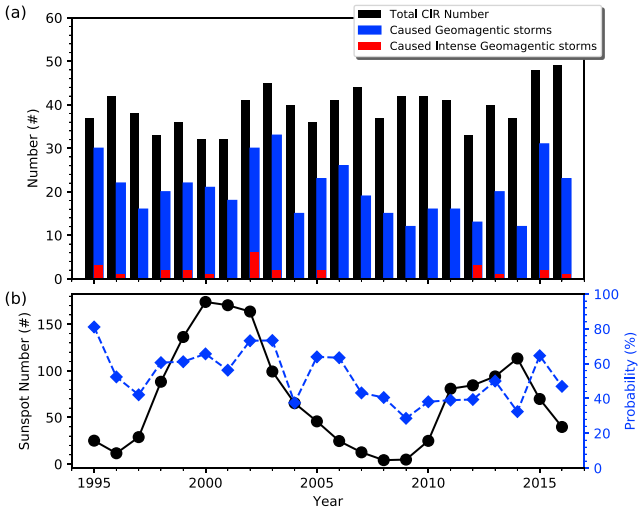

Figure 2. The annual numbers of stream interaction regions (SIRs; black bars), the annual numbers of geomagnetic storms (blue bars), and intense geomagnetic storms (red bars) caused by SIRs (a), the annual sunspot numbers (black circles) and the possibilities of SIRs causing geomagnetic storms (hollow blue circles) in each year (b) from 1995 to 2016.The error bars show 1σ uncertainties calculated by $\sqrt{\frac{P(1-P)}{N}}$, where P is the ratio and N is the total number of SIRs in each year. CIR = corotating interaction region.

compressed proton number density, increased temperature, and continuously increased solar wind speed are indicated in this region.

Finally, we identified 290 SIRs from 2010 to 2016 based on the Wind observations. Combined with 576 SIRs in the JL catalog, a total of 866 SIRs were observed near the Earth from 1995 to 2016. This extended SIR catalog is shown as a supporting information table in this paper. It should be noted that some SIRs in the JL catalog were obtained based on ACE observations. Because the increasing velocity profile and the enhanced magnetic field strength are the important criteria in determining the boundaries of SIRs, the edges of some SIRs may be different between Wind and ACE observations. Considering the differences in Wind and ACE orbits, we checked whether the boundaries determined from the ACE data are consistent with those obtained from the Wind spacecraft data. According to the observations from the Wind spacecraft, we manually made some minor corrections to the times of the SIR boundaries in the JL catalog. Such modifications are usually less than half an hour.

The occurrence of SIR, CIR, or HHS during the solar cycle has been widely examined. For example, Legrand and Simon (1989) classified geomagnetic storms according to their interplanetary sources and found that solar wind velocity, density, and temperature contribute to geomagnetic activity. Feynman and Yue Gu (1986) reported corotating HHSs occur more often during the descending phase of the solar cycle. In agreement with the earlier findings, the occurrence of HHSs, which are recognized as drivers of SIRs, increased during the descending phase of a solar cycle (Bame et al., 1976; Tsurutani et al., 1995). The annual numbers of SIRs from 1995 to 2009 have been discussed by Jian et al. (2006) and Jian et al. (2011). They found that the SIR occurrence rate was generally higher in the descending phase of solar cycle 23. In this work, we survey the SIRs in two solar cycles (1995–2016) to reconfirm this conclusion. The annual numbers of SIRs are denoted by the black bars in Figure 2a. Over the 20 years of the study period, the annual number of SIRs varied from 32 to 49, with an average annual SIR event number of 39. These numbers are larger than the annual numbers of ICMEs, as shown in Chi et al. (2016). To illustrate the solar cycle variations of SIR occurrence, the black symbols in Figure 2b denote the annual sunspot numbers from 1995 to 2016. During the declining phase of the two solar cycles, especially for solar cycle 24, the occurrences of SIRs are higher than those in other phases.

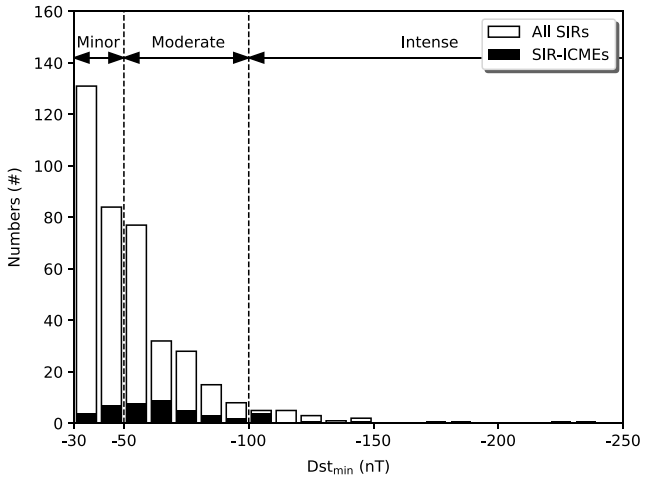

Figure 3. Distribution of number of stream interaction regions against the minimum value of the *Dst* index (Dst_{min}).

Table 1
The Numbers and Probabilities of SIRs Caused Different Levels Geomagnetic Storms

All storm	Minor storm	Moderate storm	Intense storm
453 (52%)	240 (28%)	187 (22%)	26 (3%)

The maximum occurrence of SIRs occurs in 2016, which is in the declining phase of solar cycle 24. This finding confirms the previous results suggested by Bame et al. (1976), Jian et al. (2011), and Yermolaev et al. (2012).

3. Geoeffectiveness of SIRs

To check the geoeffectiveness of SIRs, the *Dst* indices from the World Data Center are used to check the minimum intensities of the possible geomagnetic storms associated with the SIRs. Similar to the method we used in Shen et al. (2017), if an SIR has the dominant contribution in producing the minimum value of the *Dst* index (Dst_{min}) and Dst_{min} is ≤ -30 nT, we defined that storm as an SIR-associated geomagnetic storm. In total, during 1995–2016, 453 geomagnetic storms were associated with SIRs and their associated structures. Therefore, 52% of the SIRs were able to produce geomagnetic storms. Previous results show that 58% of the ICMEs could produce geomagnetic storms(e.g., Shen et al., 2017, and references therein). Thus, the possibility of SIRs causing geomagnetic storms is similar but slightly lower than that of ICMEs. Furthermore, we categorized the geomagnetic storms into minor geomagnetic storms (-50 nT $< Dst_{min} \leq -30$ nT), moderate geomagnetic storms (-100 nT $< Dst_{min} \leq -50$ nT) and intense geomagnetic storms ($Dst_{min} \leq 100$ nT). The white bars in Figure 3 show the distribution of numbers of SIRs against the minimum value of the *Dst* index (Dst_{min}). The majority of the SIR events exhibit Dst_{min} values larger than -100 nT and the distribution peaks at ~ -30 nT. The numbers and percentage of SIRs followed by each type of geomagnetic storms are tabulated in Table 1. Based on Table 1, approximately 94% of the SIR events that cause geomagnetic storms are associated with minor geomagnetic storms (53%) and moderate geomagnetic storms (41%) together, and only 6% of geomagnetic storm-inducing SIR events are able to produce intense geomagnetic storms. In agreement with the earlier findings, SIRs drive mostly minor to moderate geomagnetic storms (e.g., Mustajab et al., 2011; Tsurutani et al., 1995).

Previous results suggested that the properties of SIRs tend to have different properties in different solar phases (e.g.,González-Esparza & Smith, 1997; Riley, Linker, Lionello, & Mikic, 2012; Riley, Linker, Americo Gonzalez-Esparza, et al., 2012, and references therein). The annual averages of P_{max}, B_{max}, and V of SIRs have similar solar cycle variations, which may cause variations in geoeffectiveness in different solar phases. To study such a variation, blue bars in Figure 2a exhibit the annual numbers of geomagnetic storms caused by SIRs. From 1995 to 2016, the average numbers of geomagnetic storms caused by SIRs is 20, which is larger than that caused by ICMEs. The reason is that the annual numbers of SIRs are larger than ICMEs. The annual number of geomagnetic storms caused by SIRs is highest in 2003, which is in the descending phase of solar cycle 23. In that year, SIRs caused 33 geomagnetic storms with $Dst_{min} \leq -30$ nT. In contrast, SIRs only caused 10 geomagnetic storms in 2009. Furthermore, there are other two peaks located in 1995 and 2015, which correspond to the descending phases of solar cycles 22 and 24. These results reconfirm that the number of geomagnetic storms caused by SIRs is higher in the solar descending phase (e.g., Bame et al., 1976; Feynman & Yue Gu, 1986; Tsurutani et al., 1995). The hollow blue circles in Figure 2b show the annual probabilities of geoeffective SIRs. The error bars show 1σ uncertainties calculated by $\sqrt{\frac{P(1-P)}{N}}$, where P is the ratio and N is the total number of SIRs in each year. In 1995, 2003, and 2015, more than 70% of the SIRs caused geomagnetic storms. In particular, in 1995, approximately 80% of the SIRs were able to produce geomagnetic storms. These results further confirm that SIRs are more geoeffective in the solar descending phase (e.g., Gonzalez et al., 1999; Tsurutani et al., 1995). In addition, the probabilities of SIRs causing geomagnetic storms in solar cycle 24 are slightly smaller than those in solar cycle 23. One possible reason is that the magnetic field, especially the south component of the magnetic field of SIRs in solar cycle 24 was weaker than that in solar cycle 23 (e.g., Gopalswamy et al., 2014; Jian et al., 2011, and references therein).

In the present study, only 26 intense geomagnetic storms are driven by SIRs. Therefore, only 3% of the SIRs could generate intense geomagnetic storms. As suggested by Shen et al. (2017), 20% of ICMEs can generate intense geomagnetic storms. This finding confirms the previous results demonstrating that the geoeffectiveness of SIRs is weaker than that of ICMEs because of the highly oscillatory nature of the GSM magnetic field z component (Tsurutani et al., 2006). Table 2 lists the times and the related Dst_{min} values for these events. Based on Table 2, the most intense geomagnetic storm caused by SIRs is the 21 October 1999 event. This was a super intense geomagnetic storm. The Dst_{min} value for this event was -237 nT. Figure 4 shows the Wind in situ observations of this SIR. The two vertical blue lines show the front and trailing edges of the SIR. Unlike the normal SIR shown in Figure 1, from 21 October 1999 09:41 UT to 22 October 1999 06:38 UT (shown as the shaded

Table 2
The List of the Intense Geomagnetic Storms With $Dst_{min} \leq -100$ nT caused by SIRs from 1995 to 2016

No	SIR begin time	SIR end time	Dst_{min}	*Dst* peak time	Interacted with ICMEs?
1	1995-3-25T22:00:00	1995-3-27T21:00:00	−107	1995-3-26T18:00:00	N
2	1995-4-7T01:49:17	1995-4-7T20:47:08	−149	1995-4-7T19:00:00	N
3	1995-10-18T10:42:00	1995-10-20T14:00:00	−127	1995-10-19T00:00:00	Y
4	1996-10-21T20:00:00	1996-10-23T08:00:00	−105	1996-10-23T05:00:00	N
5	1998-3-9T21:00:00	1998-3-11T04:00:00	−116	1998-3-10T21:00:00	N
6	1998-8-5T20:00:00	1998-8-8T04:00:00	−138	1998-8-6T12:00:00	N
7	1999-1-13T10:47:00	1999-1-15T07:00:00	−112	1999-1-14T00:00:00	N
8	1999-10-21T02:21:00	1999-10-22T13:00:00	−237	1999-10-22T07:00:00	Y
9	2000-5-23T14:00:00	2000-5-24T14:00:00	−147	2000-5-24T09:00:00	N
10	2002-5-11T10:30:00	2002-5-12T14:00:00	−110	2002-5-11T20:00:00	N
11	2002-9-3T02:00:00	2002-9-4T19:00:00	−109	2002-9-4T06:00:00	N
12	2002-9-30T08:02:08	2002-10-2T12:00:00	−176	2002-10-1T17:00:00	Y
13	2002-10-7T00:00:00	2002-10-8T06:00:00	−115	2002-10-7T08:00:00	N
14	2002-10-14T03:57:51	2002-10-16T02:53:34	−100	2002-10-14T14:00:00	N
15	2002-11-20T10:49:00	2002-11-21T13:00:00	−128	2002-11-21T11:00:00	N
16	2003-6-18T04:42:00	2003-6-19T04:00:00	−141	2003-6-18T10:00:00	Y
17	2003-7-11T00:00:00	2003-7-12T20:00:00	−105	2003-7-12T06:00:00	N
18	2005-8-23T19:27:00	2005-8-24T17:55:00	−184	2005-8-24T12:00:00	Y
19	2005-8-30T18:05:00	2005-9-1T04:00:00	−122	2005-8-31T20:00:00	N
20	2012-4-23T02:08:34	2012-4-26T00:32:08	−108	2012-4-24T05:00:00	Y
21	2012-10-8T04:17:08	2012-10-10T00:59:59	−105	2012-10-9T09:00:00	Y
22	2012-11-12T15:08:34	2012-11-14T21:00:00	−108	2012-11-14T08:00:00	Y
23	2013-5-31T15:06:25	2013-6-2T02:47:08	−119	2013-6-1T09:00:00	N
24	2015-3-15T22:45:00	2015-3-18T17:30:00	−223	2015-3-17T23:00:00	Y
25	2015-10-7T02:34:17	2015-10-7T23:21:25	−124	2015-10-7T23:00:00	N
26	2016-1-19T07:39:54	2016-1-23T13:42:51	−104	2016-1-20T17:00:00	Y

Note. Dates are formatted as year-month-day.SIR = stream interaction region; ICME = interplanetary coronal mass ejection.

region), the Wind observations exhibit obvious signatures of an ICME, including an enhanced magnetic field, smooth rotated magnetic field, bidirectional electron beam, and low plasma beta. This ICME was listed in Jian's ICME catalog Jian et al. (2006), Richardson and Cane's ICME catalog (Richardson & Cane, 2010), and USTC's ICME catalog (Chi et al., 2016). This event represented interaction between an SIR and an ICME and has been studied by Dal Lago et al. (2006). Dal Lago et al. (2006) analyzed the solar origination of this interaction structure in detail. They found that the halo CME, which was first observed by SOHO/LASCO C2 at 18 October 1999 00:06 UT, was the solar source of the ICME. In addition, the fast solar wind stream from a coronal hole beside the source region of this CME caught up with and compressed it. At the trailing edge of the ICME embedded in the SIR, the magnetic field, especially the south component of the magnetic field, was clearly enhanced obviously due to the compression between the ICME and the SIR. Based on the variation in the *Dst* indices, this compressed region, with a stronger south component of the magnetic field, was the main cause of this intense geomagnetic storm. Thus, we think that the interaction between the SIR interacted and the ICME was an important factor in causing this intense geomagnetic storm. SIRs interacting with ICMEs might form complex structures, which have been named compound streams or hybrid events (e.g., Burlaga, 1975; Dal Lago et al., 2006; Jian et al., 2006). In the following analysis, we call such events *SIR-ICME* events to clarify that these structures form through the interaction between SIRs and ICMEs. To further explore the importance of such interaction on the geoeffectiveness of SIRs, we check all intense geomagnetic storms caused by SIRs in our catalog. The last column in Table 2 indicates whether the SIRs interacted with an ICME. Symbol *Y* means that this SIR interacted with an ICME, while *N* means that this SIR was not associated with any ICME. As Table 2 shows, 10 (39%) SIRs that caused intense geomagnetic storms interacted with ICMEs. Furthermore, the top four geo-

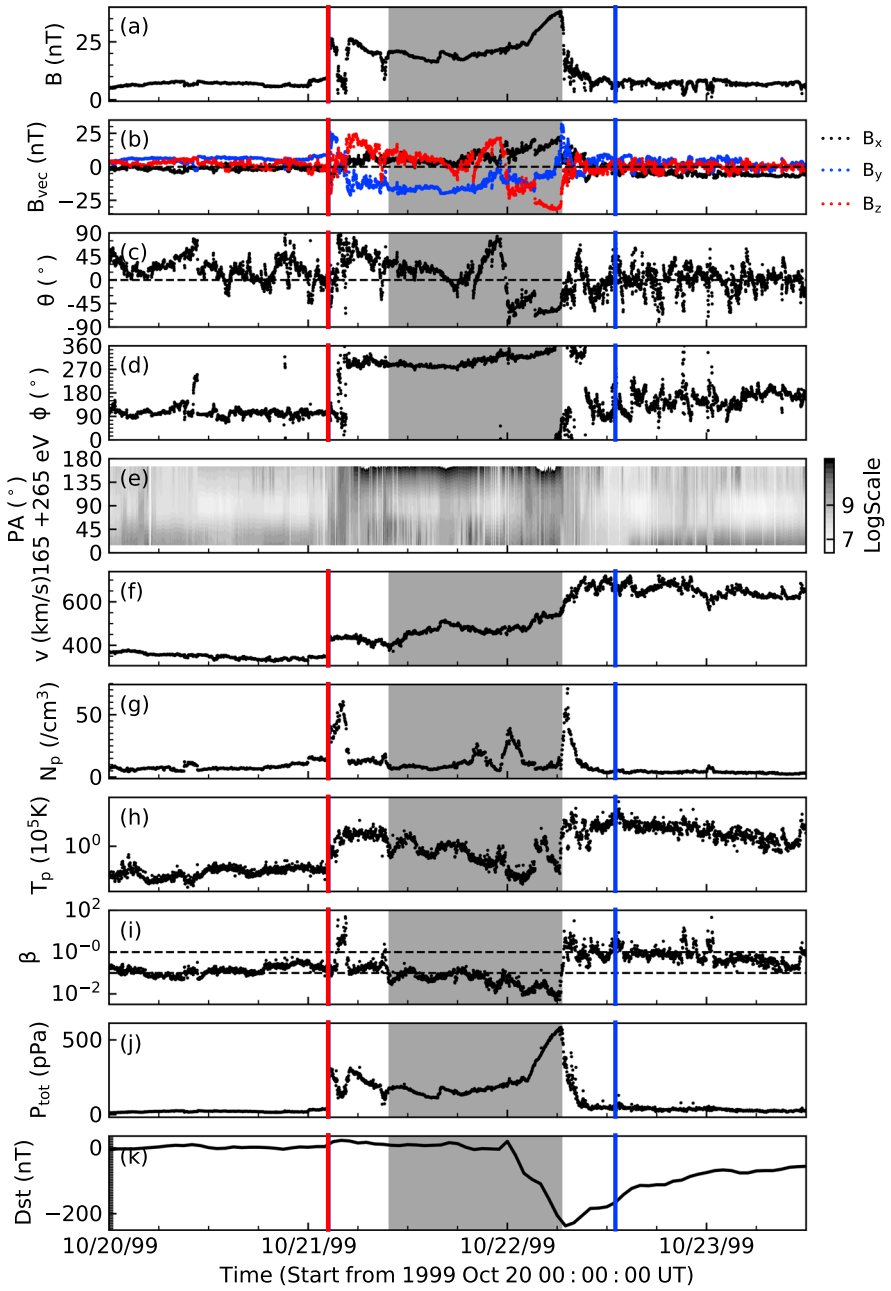

Figure 4. The Wind in situ observations and the Dst observations from 20 October 1999 12:00 to 22 October 1999.

magnetic storms in the SIR catalog, including two super intense geomagnetic storms with $Dst_{min} \leq -200$ nT, were all caused by SIR-ICME interaction structures. These results suggest that SIR-ICME structures are important sources of intense geomagnetic storms. For the events without interaction with ICMEs, the most intense geomagnetic storm is the 7 April 1995 event. The Dst_{min} value for this event was −149 nT. If we exclude the SIR-ICME interaction events, only 16 (2%) isolated SIRs caused intense geomagnetic storms.

4. Geoeffectiveness of SIR-ICME Interaction Structures

In section 3, we found that 10 intense geomagnetic storms in the SIR catalog were caused by the interaction between SIRs and ICMEs. In particular, two super intense geomagnetic storms were caused by such interactions. We suggest that the interaction between SIRs and ICMEs can enhance their geoeffectiveness. However, how significantly can the interaction between an ICME and an SIR enhance their geoeffectiveness? To answer

Table 3
The List of the SIR-ICME Interaction Events From 1995 to 2016

No	SIR begin time	SIR end time	Dst_{min}	*Dst* peak time	ICMEs begin time	ICME end time
1	1995-10-18T10:42:00	1995-10-20T14:00:00	−127	1995-10-19T00:00:00	1995-10-18T19:00:00	1995-10-19T23:08:34
2	1995-12-15T04:37:00	1995-12-17T18:00:00	−44	1995-12-16T06:00:00	1995-12-15T15:04:17	1995-12-16T19:04:17
3	1996-7-1T12:20:00	1996-7-4T02:00:00	—	1996-7-2T03:00:00	1996-7-1T17:15:00	1996-7-2T10:16:29
4	1996-8-8T00:00:00	1996-8-10T12:00:00	—	1996-8-9T23:00:00	1996-8-7T11:42:00	1996-8-8T08:14:59
5	1997-1-10T00:52:00	1997-1-11T09:00:00	−78	1997-1-10T10:00:00	1997-1-10T04:41:15	1997-1-11T02:57:45
6	1997-9-2T22:37:00	1997-9-4T05:00:00	−98	1997-9-3T23:00:00	1997-9-3T13:45:00	1997-9-3T20:40:30
7	1998-3-24T10:00:00	1998-3-27T23:00:00	−56	1998-3-25T17:00:00	1998-3-25T16:11:48	1998-3-26T09:10:41
8	1998-5-7T08:00:00	1998-5-8T18:00:00	−56	1998-5-8T21:00:00	1998-5-7T12:55:42	1998-5-7T21:17:08
9	1998-6-14T14:00:00	1998-6-16T10:00:00	—	1998-6-15T10:00:00	1998-6-14T02:20:37	1998-6-14T23:20:37
10	1999-8-9T21:30:00	1999-8-12T02:00:00	—	1999-8-11T03:00:00	1999-8-9T10:18:56	1999-8-10T16:15:00
11	1999-8-23T12:11:00	1999-8-24T20:00:00	−63	1999-8-23T16:00:00	1999-8-21T15:18:00	1999-8-23T14:06:00
12	1999-10-21T02:21:00	1999-10-22T13:00:00	−237	1999-10-22T07:00:00	1999-10-21T09:41:15	1999-10-22T06:37:30
13	1999-11-21T14:00:00	1999-11-24T06:40:00	−50	1999-11-24T10:00:00	1999-11-23T06:52:29	1999-11-23T19:41:15
14	2000-3-31T18:00:00	2000-4-2T13:00:00	−49	2000-4-2T01:00:00	2000-3-31T03:09:00	2000-4-1T07:12:00
15	2000-4-18T16:00:00	2000-4-20T02:00:00	—	2000-4-20T03:00:00	2000-4-18T20:33:00	2000-4-19T02:19:30
16	2000-5-12T15:00:00	2000-5-13T23:00:00	—	2000-5-13T04:00:00	2000-5-13T17:14:37	2000-5-14T11:48:05
17	2000-7-31T15:00:00	2000-8-2T02:00:00	−41	2000-8-2T06:00:00	2000-7-31T23:26:31	2000-8-1T12:54:43
18	2000-9-16T18:30:00	2000-9-17T23:21:25	−68	2000-9-17T00:00:00	2000-9-17T23:26:15	2000-9-21T08:37:30
19	2001-3-03T11:21:45	2001-3-6T00:00:00	−73	2001-3-5T03:00:00	2001-3-04T16:09:45	2001-3-5T02:57:45
20	2001-6-18T02:07:00	2001-6-20T05:00:00	−61	2001-6-18T09:00:00	2001-6-19T00:40:30	2001-6-19T14:24:00
21	2001-9-14T18:00:00	2001-9-15T19:00:00	—	2001-9-15T20:00:00	2001-9-14T04:55:52	2001-9-14T23:35:15
22	2001-10-11T16:48:25	2001-10-12T08:25:42	−70	2001-10-11T20:00:00	2001-10-12T03:38:26	2001-10-12T08:19:41
23	2002-9-30T08:02:08	2002-10-2T12:00:00	−176	2002-10-1T17:00:00	2002-9-30T22:03:00	2002-10-01T18:45:00
24	2002-12-19T00:25:42	2002-12-19T21:00:00	−72	2002-12-19T21:00:00	2002-12-18T15:59:15	2002-12-19T03:19:52
25	2002-12-22T10:17:08	2002-12-23T10:30:00	−67	2002-12-23T12:00:00	2002-12-21T07:12:00	2002-12-22T18:09:00
26	2003-6-18T04:42:00	2003-6-19T04:00:00	−141	2003-6-18T10:00:00	2003-6-17T19:03:00	2003-6-18T09:04:30
27	2003-8-5T18:00:00	2003-8-6T16:00:00	−60	2003-8-6T07:00:00	2003-8-5T01:59:15	2003-8-6T01:43:30
28	2004-4-5T08:00:00	2004-4-7T00:00:00	−62	2004-4-5T20:00:00	2004-4-04T02:44:15	2004-4-5T19:40:42
29	2005-8-23T19:27:00	2005-8-24T17:55:00	−184	2005-8-24T12:00:00	2005-8-24T17:55:30	2005-8-25T12:45:00
30	2006-9-30T02:10:00	2006-10-1T08:51:00	−51	2006-10-1T06:00:00	2006-9-30T09:08:37	2006-9-30T19:43:52
31	2007-12-26T10:17:08	2007-12-28T08:34:17	—	2007-12-27T15:00:00	2007-12-25T19:03:00	2007-12-26T07:39:00
32	2009-1-25T21:19:00	2009-1-29T16:00:00	−32	2009-1-26T15:00:00	2009-1-26T04:59:15	2009-1-26T14:51:00
33	2009-6-28T11:00:00	2009-6-29T14:00:00	—	2009-6-29T00:00:00	2009-6-27T18:36:00	2009-6-28T16:03:00
34	2009-8-5T04:44:00	2009-8-6T19:16:00	−39	2009-8-6T08:00:00	2009-8-5T12:31:30	2009-8-6T05:55:30
35	2010-5-29T14:55:42	2010-6-1T19:42:51	−58	2010-5-30T21:00:00	2010-5-28T19:43:30	2010-5-29T16:57:00
36	2011-2-4T01:59:59	2011-2-5T05:15:00	−63	2011-2-4T22:00:00	2011-2-4T09:29:15	2011-2-4T20:57:50
37	2011-2-14T15:12:51	2011-2-15T02:38:34	−40	2011-2-14T23:00:00	2011-2-14T18:47:08	2011-2-15T02:38:34
38	2011-5-26T14:00:00	2011-5-29T20:30:00	−80	2011-5-28T12:00:00	2011-5-28T05:33:00	2011-5-28T21:54:00
39	2011-6-4T20:08:34	2011-6-5T02:04:17	−45	2011-6-5T06:00:00	2011-6-5T01:57:00	2011-6-5T18:18:00
40	2011-11-7T06:57:51	2011-11-8T21:51:25	—	2011-11-8T16:00:00	2011-11-7T16:38:26	2011-11-7T22:38:26

this question, we combine the ICME list obtained by Chi et al. (2016) based on the Wind observations and our SIR catalog to obtain all SIR-ICME interaction events during this period. For each SIR, we first checked whether its time interval overlapped with any ICME in the ICME catalog. If there was a temporal overlap between the SIR and an ICME, we used the in situ observations to manually check if there was physical interaction between these two structures. In total, we found 60 SIR-ICME interaction events. Table 3 lists the detailed information of these events.

Table 3 *(continued)*

No	SIR begin time	SIR end time	Dst_{min}	*Dst* peak time	ICMEs begin time	ICME end time
41	2012-3-15T04:55:42	2012-3-15T20:51:25	−74	2012-3-15T21:00:00	2012-3-15T21:00:00	2012-3-16T10:30:00
42	2012-4-23T02:08:34	2012-4-26T00:32:08	−108	2012-4-24T05:00:00	2012-4-23T16:43:18	2012-4-24T02:52:30
43	2012-6-2T15:12:51	2012-6-4T23:47:08	−32	2012-6-3T20:00:00	2012-6-2T14:54:00	2012-6-03T11:06:00
44	2012-10-8T04:17:08	2012-10-10T00:59:59	−105	2012-10-9T09:00:00	2012-10-8T17:22:30	2012-10-09T13:27:11
45	2012-11-12T15:08:34	2012-11-14T21:00:00	−108	2012-11-14T08:00:00	2012-11-13T07:43:30	2012-11-14T02:24:00
46	2013-4-30T08:53:34	2013-5-1T21:25:42	−67	2013-5-1T19:00:00	2013-4-30T12:00:00	2013-4-30T22:17:08
47	2013-5-22T19:17:08	2013-5-28T02:53:34	−54	2013-5-25T07:00:00	2013-5-26T00:00:00	2013-5-26T23:06:00
48	2013-7-09T09:40:42	2013-7-11T02:55:42	−47	2013-7-10T22:00:00	2013-7-10T19:56:09	2013-7-11T02:17:48
49	2014-4-29T13:59:59	2014-5-1T19:25:42	−64	2014-4-30T10:00:00	2014-4-29T19:27:45	2014-4-30T16:03:00
50	2014-6-7T16:10:42	2014-6-8T19:36:25	−35	2014-6-8T07:00:00	2014-6-8T19:03:00	2014-6-10T10:03:00
51	2015-3-15T22:45:00	2015-3-18T17:30:00	−223	2015-3-17T23:00:00	2015-3-17T13:08:34	2015-3-17T23:21:25
52	2015-3-31T07:42:51	2015-4-5T21:42:51	—	2015-4-4T01:00:00	2015-3-31T18:07:25	2015-4-1T09:52:15
53	2015-5-18T00:12:51	2015-5-19T14:04:17	−44	2015-5-19T04:00:00	2015-5-18T22:36:25	2015-5-19T01:55:42
54	2015-8-15T08:08:34	2015-8-17T12:12:51	−84	2015-8-16T08:00:00	2015-8-15T20:42:51	2015-8-16T06:51:25
55	2015-8-28T13:25:42	2015-8-30T02:23:34	−84	2015-8-28T19:00:00	2015-8-27T09:00:00	2015-8-28T17:17:08
56	2016-1-19T07:39:54	2016-1-23T13:42:51	−104	2016-1-20T17:00:00	2016-1-19T11:16:09	2016-1-20T09:40:00
57	2016-2-2T00:42:08	2016-2-06T09:56:41	−52	2016-2-3T05:00:00	2016-2-2T20:51:25	2016-2-3T04:00:00
58	2016-3-5T02:54:11	2016-3-7T03:51:25	−96	2016-3-6T22:00:00	2016-3-5T18:08:34	2016-3-6T10:17:08
59	2016-7-19T23:08:34	2016-7-20T07:00:00	—	2016-7-20T07:00:00	2016-7-20T12:47:08	2016-7-22T15:19:17
60	2016-8-2T04:42:51	2016-8-3T12:34:17	−51	2016-8-3T11:00:00	2016-8-2T14:38:34	2016-8-3T01:12:51

Note. Dates are formatted as year-month-day. SIR = stream interaction region; ICME = interplanetary coronal mass ejection.

As discussed in section 3, 10 SIR-ICME interaction structures caused intense geomagnetic storms with $Dst_{min} \leq -100$ nT. Furthermore, by checking the associated geomagnetic activity, we found that 49 of the SIR-ICME events caused geomagnetic activities with $Dst_{min} \leq -30$ nT. Thus, 82% of the SIR-ICME events were able to produce geomagnetic storms and 17% of the SIR-ICME events were responsible for intense geomagnetic storms. The black bars in Figure 3 show the distribution of the Dst_{min} of the geomagnetic storms caused by the SIR-ICME events. Compared with all SIRs, the distribution for SIR-ICME events has an obvious rightward shift. The peak is located near −60 nT. Therefore, the geoeffectiveness of SIR-ICME events is greater than that of SIR events. Furthermore, in Figure 5, the black, purple, green, and blue horizontal lines show the probabilities of causing geomagnetic storms for all SIRs, isolated ICMEs (I-ICME), SIR-ICME interaction structures, and shock-ICME interaction structures (S-ICMEs), respectively. The vertical extent of each box shows the 1σ uncertainties. The probabilities for I-ICMEs and S-ICMEs are directly adopted from Shen et al. (2017). The geoeffectiveness of SIR-ICME interaction structures is obviously greater than those of all SIRs and I-ICMEs. The probability of the SIR-ICME interaction structures causing geomagnetic storms is almost the same as that of the S-ICMEs. This result indicates that the interaction between SIRs and ICMEs can significantly enhance the SIR geoeffectiveness. This process might be another way to enhance the geoeffectiveness of ICMEs in addition to the interaction between multiple ICMEs and shock compression of ICMEs (e.g., Lugaz et al., 2015; Shen et al., 2017; Wang, Ye, Wang, & Xiong, 2003; Wang, Ye, Wang, & Xue, 2003, and references therein). A possible reason is that a fast stream compressing an ICME can enhance the magnetic field intensity in the ICME, thereby enhancing the geoeffectiveness of the ICME. However, as shown in Figure 5, the interaction between SIRs and ICMEs did not significantly enhance the possibility of causing intense geomagnetic storms. The probability of SIR-ICME interaction structures causing an intense geomagnetic storm is 16%, which is similar to that of I-ICMEs but much lower

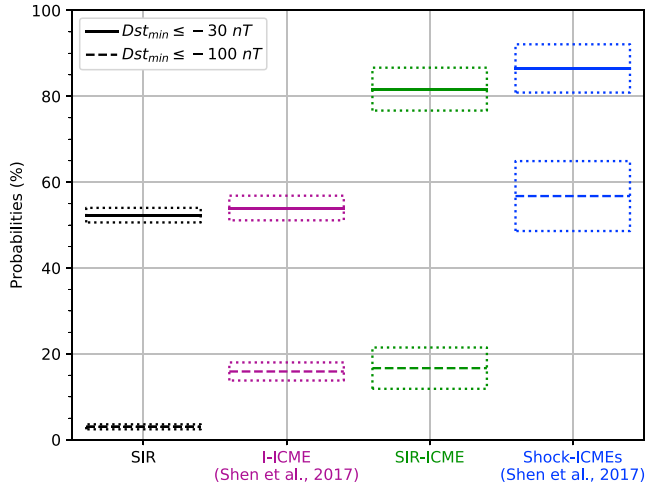

Figure 5. Probabilities of different structures causing geomagnetic storms and intense geomagnetic storms. The vertical extent of each box shows the 1σ uncertainties calculated by $\sqrt{\frac{P(1-P)}{N}}$, where the P is the probability while N is the total number of the examples in each group.

than that for S-ICMEs. Therefore, SIR-ICME interaction process may enhance the probability of causing geomagnetic storms but has little effect on the event's capacity to cause intense geomagnetic storms. A possible reason is that the compression between a SIR and a ICME is weaker than that of the shock compression process. Thus, an intense B_s, which is the necessary condition of interplanetary structures in causing intense geomagnetic storms, is difficult to achieve satisfaction in the SIR-ICME interactive process. Another possible reason is the B_s duration. The duration of the B_s is an important factor deciding the geoeffectiveness of the solar wind (Lockwood et al., 2016). The duration of B_s in SIR-ICME events is longer than in SIRs or CMEs in isolation and may cause the SIR-ICME events to be more geoeffective.

5. Conclusions and Discussion

In this work, the geoeffectiveness of SIRs from 1995 to 2016 has been studied based on an extended SIR catalog. This SIR catalog is the combination of the JL catalog from 1995 to 2009 and a newly developed catalog using the Wind in situ observations from 2010 to 2016. Based on the analysis of the 866 SIR events over the 22 years, we find the following:

1. Approximately 52% of the SIRs caused geomagnetic storms with $Dst_{\min} \leq -30$ nT. The geoeffectiveness values for SIRs and ICMEs are similar. However, only 3% of the SIRs caused intense geomagnetic storms with $Dst_{\min} \leq -100$ nT, indicating that the probability of SIRs causing intense geomagnetic storms is much smaller than that of ICMEs. It should be noted that the number of geomagnetic storms caused by SIRs is higher than that caused by ICMEs because of the larger number of SIRs. This confirms the previous results obtained by Yermolaev et al. (2012), and Echer et al., 2008 (2008, 2013).

   Due to the highly oscillatory nature of the GSM magnetic field *z* component, the resultant storms of SIRs are usually weak to moderate (Tsurutani et al., 2006). The recurrent weak and moderate storms driven by SIRs pose a problem for space-based assets, particularly at geosynchronous orbit, because these storms have long durations, hot plasma sheets, and strong spacecraft charging (Borovsky & Denton, 2006). Thus, these events have a considerable impact on global navigational satellite systems, which provide geospatial positioning to many devices autonomously. By checking the probability of an SIR causing a geomagnetic storm, we conclude that SIRs are more likely to cause geomagnetic storms (70%) in the descending phase of the solar cycle. In agreement with previous findings, SIRs must be carefully considered in the forecasting of geomagnetic storms especially in the solar descending phase (Gonzalez et al., 1999; Jian et al., 2011; Tsurutani et al., 1995).

   The ratios of geomagnetic storm-inducing SIRs in this work are similar to the results obtained by Alves et al. (2006) but much lower than those obtained by Zhang et al. (2008). Zhang et al. (2008) found that 82% of *pure* SIRs caused geomagnetic storms. The possible reason for this difference is that the definition of SIRs is different. Zhang et al. (2008) used the Hakamada-Akasofu-Fry method to obtain their SIR list and obtained only 159 pure SIRs from 1996 to 2005. In the same period, we identified a total of 454 SIRs. Thus, the number of SIRs in our catalog is much larger than Zhang et al. (2008). Hence, the criteria used in Zhang et al. (2008) to determine SIRs are much stricter than ours.
2. By investigating the 26 intense geomagnetic storms caused by SIRs, we found that 10 of them were caused by interaction structures between SIRs and ICMEs. Thus, only 16 intense geomagnetic storms were caused by isolated SIRs. We suggest that SIR-ICME events might be another important source of geomagnetic storms. In addition, 60 SIR-ICME interaction events occurred from 1995 to 2016, of which 49 caused geomagnetic storms and 10 caused intense geomagnetic storms. Furthermore, we quantitatively compared the geoeffectiveness of different interplanetary structures of SIRs, I-ICMEs, SIR-ICME events, and S-ICMEs events. The comparison results show that the interaction process between SIRs and ICMEs enhances the possibility of causing geomagnetic storms. However, this interaction process does not enhance the probability of causing intense geomagnetic storms. Similar results have been partially suggested by Fenrich and Luhmann (1998), Webb et al. (2000), Dal Lago et al. (2006), Kilpua, Li, et al. (2012), and Kataoka et al. (2015). They found that SIRs and fast solar wind streams behind the ICMEs compress these structures and enhance their geoeffectiveness. Thus, for space weather forecasting, we should pay more attention to SIR-ICME interaction structures.

Acknowledgments
We acknowledge the use of the data from *Wind* satellites and the world data center (WDC) for Geomagnetism, Kyoto. The *Wind*/MFI, *Wind*/SWE, *Wind*/SFPD, and *Wind*/3DP data are downloaded from the NASA's Space Physics Data Facility (SPDF, http://spdf.gsfc.nasa.gov/). The *Dst* indices came from the link http://wdc.kugi.kyoto-u.ac.jp/. The yearly sunspot number data locate at Royal Observatory of Belgium via the link http://www.sidc.be/silso/datafiles. We are grateful to the 1996–2009 JL SIR list from the link http://www-ssc.igpp.ucla.edu/~jlan/ACE/Level3/SIR_List_from_Lan_Jian.pdf. This work is supported by grants from CAS (Youth Innovation Promotion Association CAS and Key Research Program of Frontier Sciences QYZDB-SSW-DQC015), NSFC (41774181 and 41474164), the Fundamental Research Funds for the Central Universities, and the Specialized Research Fund for State Key Laboratories. Y. M. is also supported by the NSFC grants(41574165 and 41774178). The authors also wish to thank the Editor M. Hapgood and two unknown referees who took the time to scrutinize carefully the successive versions of this paper and, by many suggestions, contributed to improving the final version.

References

Alves, M. V., Echer, E., & Gonzalez, W. D. (2006). Geoeffectiveness of corotating interaction regions as measured by *Dst* index. *Journal of Geophysical Research*, *111*, 1–9. https://doi.org/10.1029/2005JA011379

Astafyeva, E., Yasyukevich, Y., Maksikov, A., & Zhivetiev, I. (2014). Geomagnetic storms, super-storms, and their impacts on GPS-based navigation systems. *Space Weather*, *12*, 508–525. https://doi.org/10.1002/2014SW001072

Balogh, A., & Erdös, G. (2013). The heliospheric magnetic field. *Space Science Reviews*, *176*(1-4), 177–215. https://doi.org/10.1007/s11214-011-9835-3

Bame, S., Asbridge, J., Feldman, W., & Gosling, J. (1976). Solar cycle evolution of high-speed solar wind streams. *The Astrophysical Journal*, *207*, 977–980.

Borovsky, J. E., & Denton, M. H. (2006). Differences between CME-driven storms and CIR-driven storms. *Journal of Geophysical Research*, *111*, A07S08. https://doi.org/10.1029/2005JA011447

Borovsky, J. E., & Shprits, Y. Y. (2017). Is the *Dst* index sufficient to define all geospace storms? *Journal of Geophysical Research: Space Physics*, *122*, 11,543–11,547. https://doi.org/10.1002/2017JA024679

Burlaga, L. F. (1975). Interplanetary streams and their interaction with the earth. *Space Science Reviews*, *17*, 327–352.

Burlaga, L., Sittler, E., Mariani, F., & Schwenn, R. (1981). Magnetic loop behind an interplanetary shock: Voyager, helios, and IMP 8 observations. *Journal of Geophysical Research*, *86*, 6673–6684. https://doi.org/10.1029/JA086iA08p06673

Burlaga, L. F., Skoug, R. M., Smith, C. W., Webb, D. F., Zurbuchen, T. H., & Reinard, A. (2001). Fast ejecta during the ascending phase of solar cycle 23: ACE observations, 1998–1999. *Journal of Geophysical Research*, *106*(A), 20,957–20,978.

Cane, H. V., & Richardson, I. G. (2003). Interplanetary coronal mass ejections in the near-Earth solar wind during 1996–2002. *Journal of Geophysical Research*, *108*(A), 1156. https://doi.org/10.1029/2002JA009817

Chi, Y., Shen, C., Wang, Y., Ye, P., Xu, M., Ye, P., & Wang, S. (2016). Statistical study of the interplanetary coronal mass ejections from 1995 to 2015. *Solar Physics*, *291*(8), 2419–2439. https://doi.org/10.1007/s11207-016-0971-5

Dal Lago, A., Gonzalez, W. D., Balmaceda, L. A., Vieira, L. E., Echer, E., Guarnieri, F. L., et al. (2006). The 17–22 October (1999) solar-interplanetary-geomagnetic event: Very intense geomagnetic storm associated with a pressure balance between interplanetary coronal mass ejection and a high-speed stream. *Journal of Geophysical Research*, *111*, 1–5. https://doi.org/10.1029/2005JA011394

Echer, E., Gonzalez, W., Tsurutani, B., & Gonzalez, A. (2008). Interplanetary conditions causing intense geomagnetic storms ($Dst \leq -100$ nT) during solar cycle 23 (1996–2006). *Journal of Geophysical Research*, *113*, A05221.

Echer, E., Tsurutani, B. T., & Gonzalez, W. D. (2013). Interplanetary origins of moderate (-100 nT $< Dst \leq -50$ nT) geomagnetic storms during solar cycle 23 (1996–2008). *Journal of Geophysical Research: Space Physics*, *118*, 385–392. https://doi.org/10.1029/2012JA018086

Fenrich, F. R., & Luhmann, J. (1998). Geomagnetic response to magnetic clouds of different polarity. *Geophysical Research Letters*, *25*(15), 2999–3002. https://doi.org/10.1016/0032-0633(87)90159-0

Feynman, J., & Yue Gu, X. (1986). Prediction of geomagnetic activity on time scales of one to ten years. *Reviews of Geophysics*, *24*(3), 650–666.

Gonzalez, W. D., Joselyn, J. A., Kamide, Y., Kroehl, H. W., Rostoker, G., Tsurutani, B. T., & Vasyliunas, V. M. (1994). What is a geomagnetic storm? *Journal of Geophysical Research*, *99*(A4), 5771–5792.

Gonzalez, W. D., Tsurutani, B. T., & Cláa de Gonzalez, A. L. (1999). Interplanetary origin of geomagnetic storms. *Space Science Reviews*, *88*(3-4), 529–562. https://doi.org/10.1023/A:1005160129098

González-Esparza, J. Américo, & Smith, E. J. (1996). Solar cycle dependence of the solar wind dynamics: Pioneer voyager, and Ulysses from 1 to 5 AU. *Journal of Geophysical Research*, *101*(A11), 24,359–24,371.

González-Esparza, J. Américo, & Smith, E. J. (1997). Three-dimensional nature of interaction regions: Pioneer, voyager, and Ulysses solar cycle variations from 1 to 5 AU. *Journal of Geophysical Research*, *102*(A5), 9781–9792.

Gopalswamy, N. (2006). Properties of interplanetary coronal mass ejections. *Space Science Reviews*, *124*(1), 145–168.

Gopalswamy, N., Akiyama, S., Yashiro, S., Xie, H., Mäkelä, P., & Michalek, G. (2014). Anomalous expansion of coronal mass ejections during solar cycle 24 and its space weather implications. *Geophysical Research Letters*, *41*, 2673–2680. https://doi.org/10.1002/2014GL059858

Gosling, J. T., & Pizzo, V. J. (1999). Formation and evolution of corotating interaction regions and their three dimensional structure. *Space Science Reviews*, *89*, 21–52. https://doi.org/10.1007/978-94-017-1179-1-3

Gosling, J. T., Pizzo, V., & Bame, S. J. (1973). Anomalously low proton temperatures in the solar wind following interplanetary shock waves—Evidence for magnetic bottles? *Journal of Geophysical Research*, *78*(13), 2001. https://doi.org/10.1029/JA078i013p02001

Jian, L. K., Russell, C. T., & Luhmann, J. G. (2011). Comparing solar minimum 23/24 with historical solar wind records at 1 AU. *Solar Physics*, *274*(1-2), 321–344.

Jian, L. K., Russell, C. T., Luhmann, J. G., Galvin, A. B., & Simunac, K. D. (2013). Solar wind observations at sterEO: 2007–2011. *AIP Conference Proceedings*, *1539*, 191–194. https://doi.org/10.1063/1.4811020

Jian, L., Russell, C. T., Luhmann, J. G., & Skoug, R. M. (2006). Properties of stream interactions at one AU during 1995–2004. *Solar Physics*, *239*(1-2), 337.

Jian, L. K., Russell, C. T., Luhmann, J. G., Skoug, R. M., & Steinberg, J. T. (2008). Stream interactions and interplanetary coronal mass ejections at 5.3 AU near the solar ecliptic plane. *Solar Physics*, *250*(2), 375–402. https://doi.org/10.1007/s11207-008-9204-x

Kappenman, J. G. (2005). An overview of the impulsive geomagnetic field disturbances and power grid impacts associated with the violent Sun-Earth connection events of 29–31 October 2003 and a comparative evaluation with other contemporary storms. *Space Weather*, *3*, S08C01. https://doi.org/10.1029/2004SW000128

Kataoka, R., Shiota, D., Kilpua, E., & Keika, K. (2015). Pileup accident hypothesis of magnetic storm on 17 March 2015. *Geophysical Research Letters*, *42*, 5155–5161. https://doi.org/10.1002/2015GL064816

Kilpua, E. K., Balogh, A., von Steiger, R., & Liu, Y. D. (2017). Geoeffective properties of solar transients and stream interaction regions. *Space Science Reviews*, *212*(3-4), 1271–1314. https://doi.org/10.1007/s11214-017-0411-3

Kilpua, E. K. J., Jian, L. K., Li, Y., Luhmann, J. G., & Russell, C. T. (2012). Observations of ICMEs and-like solar wind structures from 2007–2010 using near-Earth and stereo observations. *Solar Physics*, *281*, 391–409.

Kilpua, E., Koskinen, H. E. J., & Pulkkinen, T. I. (2017). Coronal mass ejections and their sheath regions in interplanetary space. *Living Reviews in Solar Physics*, *14*(1), 5. https://doi.org/10.1007/s41116-017-0009-6

Kilpua, E. K. J., Li, Y., Luhmann, J. G., Jian, L. K., & Russell, C. T. (2012). On the relationship between magnetic cloud field polarity and geoeffectiveness. *Annales Geophysicae*, *30*(7), 1037–1050. https://doi.org/10.5194/angeo-30-1037-2012

Kilpua, E. K. J., Liewer, P. C., Farrugia, C., Luhmann, J. G., Möstl, C., Li, Y., et al. (2009). Multispacecraft observations of magnetic clouds and their solar origins between 19 and 23 may 2007. *Solar Physics*, *254*(2), 325–344.

Kilpua, E. K. J., Mierla, M., Zhukov, A. N., Rodriguez, L., Vourlidas, A., & Wood, B. (2014). Solar sources of interplanetary coronal mass ejections during the solar cycle 23/24 minimum. *Solar Physics*, *289*(10), 3773–3797. https://doi.org/10.1007/s11207-014-0552-4

Legrand, J.-P., & Simon, P. A. (1989). Solar cycle and geomagnetic activity: A review for geophysicists. I-The contributions to geomagnetic activity of shock waves and of the solar wind. II-The solar sources of geomagnetic activity and their links with sunspot cycle activity. *Annales geophysicae*, *7*, 565–593.

Lockwood, M., Owens, M. J., Barnard, L. A., Bentley, S., Scott, C. J., & Watt, C. E. (2016). On the origins and timescales of geoeffective IMF. *Space Weather*, *14*, 406–432. https://doi.org/10.1002/2016SW001375

Lucas, G. M., Love, J. J., & Kelbert, A. (2018). Calculation of voltages in electric power transmission lines during historic geomagnetic storms: An investigation using realistic earth impedances. *Space Weather*, *16*, 185–195. https://doi.org/10.1002/2017SW001779

Lugaz, N., Farrugia, C. J., Smith, C. W., & Paulson, K. (2015). Shocks inside CMEs: A survey of properties from 1997 to 2006. *Journal of Geophysical Research A: Space Physics*, *120*, 2409–2427. https://doi.org/10.1002/2014JA020848

Mayaud, P. N. (2013). The *Dst* index. In *Derivation, Meaning, and Use of Geomagnetic Indices* (chap. 8, pp. 115–129). Washington, D. C.: American Geophysical Union (AGU). https://doi.org/10.1002/9781118663837.ch8

Mustajab, F., & Badruddin (2011). Geoeffectiveness of the interplanetary manifestations of coronal mass ejections and solar-wind stream–stream interactions. *Astrophysics and Space Science*, *331*(1), 91–104.

O'Brien, T., & McPherron, R. L. (2000). Forecasting the ring current index Dst in real time. *Journal of Atmospheric and Solar-Terrestrial Physics*, *62*(14), 1295–1299. https://doi.org/10.1016/S1364-6826(00)00072-9

Owens, M. J. (2005). Characteristic magnetic field and speed properties of interplanetary coronal mass ejections and their sheath regions. *Journal of Geophysical Research*, *110*, A01105. https://doi.org/10.1029/2004JA010814

Richardson, I. G., & Cane, H. V. (2010). Near-Earth interplanetary coronal mass ejections during solar cycle 23 (1996–2009): Catalog and summary of properties. *Solar Physics*, *264*, 189.

Riley, P., Linker, J. A., Americo Gonzalez Esparza, J., Jian, L. K., Russell, C. T., & Luhmann, J. G. (2012). Interpreting some properties of CIRs and their associated shocks during the last two solar minima using global MHD simulations. *Journal of Atmospheric and Solar-Terrestrial Physics*, *83*, 11–21. https://doi.org/10.1016/j.jastp.2012.01.019

Riley, P., Linker, J. A., Lionello, R., & Mikic, Z. (2012). Corotating interaction regions during the recent solar minimum: The power and limitations of global MHD modeling. *Journal of Atmospheric and Solar-Terrestrial Physics*, *83*, 1–10. https://doi.org/10.1016/j.jastp.2011.12.013

Sanchez-Garcia, E., Aguilar-Rodriguez, E., Ontiveros, V., & Gonzalez-Esparza, J. A. (2017). Geoeffectiveness of stream interaction regions during 2007–2008. *Space Weather*, *15*, 1052–1067. https://doi.org/10.1002/2016SW001559

Shen, C., Chi, Y., Wang, Y., Xu, M., & Wang, S. (2017). Statistical comparison of the ICME's geoeffectiveness of different types and different solar phases from 1995 to 2014. *Journal of Geophysical Research: Space Physics*, *122*, 5931–5948. https://doi.org/10.1002/2016JA023768

Temerin, M., & Li, X. (2002). A new model for the prediction of *Dst* on the basis of the solar wind. *Journal of Geophysical Research*, *107*(A12), 1472. https://doi.org/10.1029/2001JA007532

Thomson, A. W. P., McKay, A. J., Clarke, E., & Reay, S. J. (2005). Surface electric fields and geomagnetically induced currents in the Scottish power grid during the 30 October 2003 geomagnetic storm. *Space Weather*, *3*, S11002. https://doi.org/10.1029/2005SW000156

Tsurutani, B. T., Gonzalez, W. D., Gonzalez, A. L. C., Guarnieri, F. L., Gopalswamy, N., Grande, M., et al. (2006). Corotating solar wind streams and recurrent geomagnetic activity: A review. *Journal of Geophysical Research*, *111*, A07S01. https://doi.org/10.1029/2005JA011273

Tsurutani, B. T., Gonzalez, W. D., Gonzalez, A. L., Tang, F., Arballo, J. K., & Okada, M. (1995). Interplanetary origin of geomagnetic activity in the declining phase of the solar cycle. *Journal of Geophysical Research*, *100*(A11), 21,717–21,733.

Wang, C. B., Chao, J. K., & Lin, C. H. (2003). Influence of the solar wind dynamic pressure on the decay and injection of the ring current. *Journal of Geophysical Research*, *108*(A9), 1341. https://doi.org/10.1029/2003JA009851

Wang, Y. M., Ye, P. Z., Wang, S., & Xiong, M. (2003). Theoretical analysis on the geoeffectiveness of a shock overtaking a preceding magnetic cloud. *Solar Physics*, *216*(1-2), 295–310. https://doi.org/10.1023/A:1026150630940

Wang, Y. M., Ye, P. Z., Wang, S., & Xue, X. H. (2003). An interplanetary cause of large geomagnetic storms: Fast forward shock overtaking preceding magnetic cloud. *Geophysical Research Letters*, *30*(13), 1700. https://doi.org/10.1029/2002GL016861

Webb, D. F., Cliver, E. W., Crooker, N. U., Cyr, O. C. S., & Thompson, B. J. (2000). Relationship of halo coronal mass ejections, magnetic clouds, and magnetic storms. *Journal of Geophysical Research*, *105*(A4), 7491–7508.

Wimmer-Schweingruber, R. F., Crooker, N. U., Balogh, A., Bothmer, V., Forsyth, R. J., Gazis, P., et al. (2006). Understanding interplanetary coronal mass ejection signatures. Report of working group B. *Space Science Reviews*, *123*(1), 177–216.

Yermolaev, Y. I., Nikolaeva, N. S., Lodkina, I. G., & Yermolaev, M. Y. (2012). Geoeffectiveness and efficiency of CIR, sheath, and ICME in generation of magnetic storms. *Journal of Geophysical Research*, *117*, 1–9. https://doi.org/10.1029/2011JA017139

Zhang, J., Liemohn, M. W., Kozyra, J. U., Thomsen, M. F., Elliott, H. A., & Weygand, J. M. (2006). A statistical comparison of solar wind sources of moderate and intense geomagnetic storms at solar minimum and maximum. *Journal of Geophysical Research*, *111*, 1–13. https://doi.org/10.1029/2005JA011065

Zhang, J., Richardson, I. G., Webb, D. F., Gopalswamy, N., Huttunen, E., Kasper, J. C., et al. (2007). Solar and interplanetary sources of major geomagnetic storms ($Dst \leq -100$ nT) during 1996–2005. *Journal of Geophysical Research*, *112*, A10102.

Zhang, Y., Sun, W., Feng, X. S., Deehr, C. S., Fry, C. D., & Dryer, M. (2008). Statistical analysis of corotating interaction regions and their geoeffectiveness during solar cycle 23. *Journal of Geophysical Research*, *113*, 1–13. https://doi.org/10.1029/2008JA013095